PALEOCEANOGRAPHY, VOL. 10, NO. 3, PAGES 593-610, JUNE 1995

Sortable silt and fine sediment size/composition slicing : Parameters for palaeocurrent speed and palaeoceanography

I. N. McCave, B. Manighetti, and S. G. Robinson[1]
Department of Earth Sciences, University of Cambridge, Cambridge, England, United Kingdom

Abstract. Fine sediment size (<63 μm) is best measured by a sedimentation technique which records the whole size distribution. Repeated size measurement with intermediate steps of removal of components by dissolution, allows inference of the size distribution of the removed component as well as the residue. In this way, the size of the biogenic and lithogenic (noncarbonate) fractions can be determined. Observations of many size distributions suggest a minimum in grain size frequency curves at 8 to 10 μm. The dynamics of sediment erosion, deposition, and aggregate breakup suggest that fine sediment behavior is dominantly cohesive below 10-μm grain size, and noncohesive above that size. Thus silt coarser than 10 μm displays size sorting in response to hydrodynamic processes and its properties may be used to infer current speed. Silt that is finer than 10 μm behaves in the same way as clay (<2 μm). Useful parameters of the distribution are the 10-63 μm mean size and the percentage 10-63 μm in the fine fraction. We cannot use size distributions to distinguish the nature of the currents. Therefore, to infer water mass advection speeds (i.e., the mean kinetic energy of the flow, K_M), regions of high eddy kinetic energy (K_E) must be avoided. At the present, such abyssal regions lie under the high surface K_E of major current systems: Gulf Stream, Kuroshio, Agulhas, Antarctic Circumpolar Current, and Brazil/Falkland currents in the Argentine Basin. This is probably a satisfactory guide for the Pleistocene. With regard to the carbonate subfraction of the size spectrum, size modes due to both coccoliths and foraminiferal fragments can be recognized and analyzed, with the boundary between them again at about 10 μm. The flux of less than 10 μm carbonate, at pelagic sites above the lysocline, is another candidate for a productivity indicator.

Introduction

Use of the distribution of sediment components as a function of grain size and of size parameters for the inference of current strength has been commonplace in marine geology for sand-sized material. "Coarse-fraction" analyses (generally material >63 or >150 μm in diameter) are made on selected size fractions because the screening procedure results in greater precision (elimination of size-dependant bias) and is easy to perform using sieves. This applies particularly to shallow marine sediments and others with an appreciable sand fraction. For deep-sea pelagic and hemipelagic sediments the sand fraction is mainly biogenic (and is size-fractionated for isotopic work). Lithogenic components are usually either ice rafted or volcanic in origin. Procedures and permissible inferences for material of this size are well documented in standard texts on sedimentology and marine geology. Here we explore new ways of obtaining and interpreting compositional and size data from the fine fraction of deep-sea sediments. We use the terms "fine fraction" and "mud" to refer to the total material <63 μm; "silt" for the fraction 63 to 2 μm; and "clay" for <2 μm material.

Several attempts have been made to provide grain-size parameters that respond to changes in current strength. Traditional textural diagrams (triangles of Shepard and Folk) display gross aspects of sorting but not in a way that can be used as an index of current strength. In sand-sized sediments the characteristics of stratification and bedforms (ripples, dunes, etc.) may be used to estimate palaeocurrent strength, minimum flow speeds can be obtained from critical erosion curves, and modes of transport and shear stresses can be inferred

[1]Now at Department of Environmental and Geographical Sciences, Manchester Metropolitan University, Manchester, United Kingdom.

Paper number 94PA03039.
0883-8305/95/94PA-03039$10.00

from the shape of size distributions [*Southard and Boguchwal*, 1990; *Miller et al.*, 1977; *Middleton*, 1976; *Bridge*, 1981]. Deep-sea currents are rarely able to move quartz sand but can in places move foram sand to form dunes [e.g., *Lonsdale and Malfait*, 1974], and appropriate critical curves have also been developed for this material [*Miller and Komar*, 1977]. Such occurrences involve significant removal of finer sediments to leave a foram residue, with consequent low accumulation rates and lack of stratigraphic resolution. Periods of high current speed may therefore be inferred from sands but with the penalty of low temporal resolution. Ideally, one needs sensitive parameters from continuously deposited fine sediments. As these normally show few structures other than biological disturbance, size parameters are required.

Considerable effort in this direction has been devoted by Ledbetter and his associates [*Ledbetter*, 1979, 1986; *Johnson et al.*, 1988; *Haskell et al.*, 1991; *Haskell and Johnson*, 1993]. Their chosen instrument has been the Elzone particle counter, and favored parameter the noncarbonate silt (4 or 5.6 to 63 or 70 μm) mean size. Comparison of the late Glacial time trends shown by *Ledbetter and Balsam* [1985] and *Haskell et al.* [1991] for regions not far apart on the U.S. Eastern Margin shows a lack of congruence for inferred current speed trends of the same water mass. It is not clear whether this is due to the parameter chosen being relatively insensitive, the influence of nearby sources, a difference in the type of current recorded (eddy or mean flow), stratigraphic miscorrelation or a real spatial difference in mean flow speed. There is a need to examine all of these factors, including the parameterization of size in relation to flow speed.

One of the central problems of inferring currents from size is the influence of source. We seek to eliminate the effects of source in differing ways. One is to determine an external input function and compare deviations of the size time-trend from that of the input [*Manighetti and McCave*, this issue]. Another is to determine the carbonate and noncarbonate size trends and look for common behavior [*Wang and McCave*, 1990; *Robinson and McCave*, 1994]. However, we argue below that mixing in the delivery systems results in elimination of systematic source effects on short timescales (order of 100 ka and less).

Size Measurement of Fine Sediment Components

It is possible, by repeated size measurement of a sample with removal of components, to infer the component size distributions. Size measurement itself, however, is surprisingly widely misunderstood.

Measurement of Fine Grain Sizes

Broadly, methods of size measurement may be divided into those which yield information on the whole size distribution and those for which the information comes from a size window with upper and lower limits. Wholesale misunderstanding has arisen from attempts to attribute significance to differences in parameters obtained for the same sediment by different methods; for example when the mean or sorting from a Coulter Counter analysis with a 2 to 40 μm window is compared with a Sedigraph analysis which has a 0-63 μm window. The Coulter Counter in this case does not "see" the clay which may comprise a significant part of the size spectrum. The problems are compounded by manufacturers who make unrealistic claims for the analytical range of their instruments (see also *McCave and Syvitski* [1991] and *Syvitski* [1991]). The bottom line is the following: (1) measurements using a sedimentation principle (e.g.,

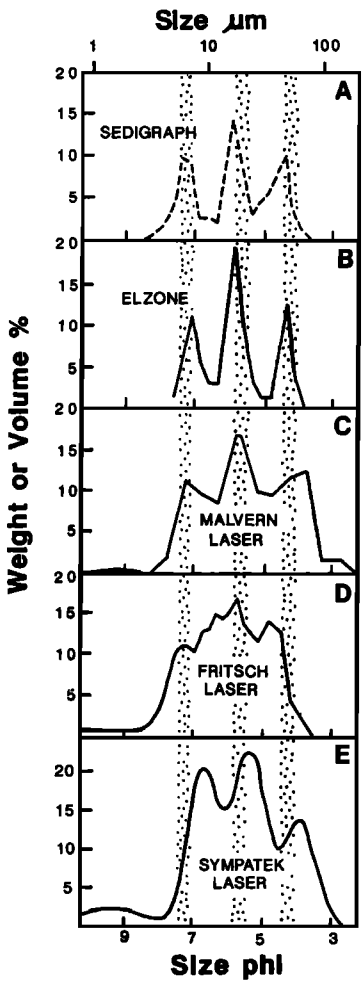

Figure 1. Examples of size distributions measured by different instruments [from *Singer et al.*, 1988, *Agrawal et al.*, 1991]

pipette method, Sedigraph) are capable of sensing the total amount of material present and giving a fairly accurate measurement of the 1 to 100 μm size distribution (but beware of montmorillonite [*Stein*, 1985]); (2) electrical sensing zone counters (Coulter, Elzone) give an accurate measurement in the 0.5 to 100 μm range, but they do not see anything outside the chosen window (e.g., 1 to 40 μm, 2 to 80 μm), in particular they miss some of the clay; (3) laser diffraction sizers (Malvern, CILAS, Horiba, Fritsch, Coulter, Sympatek) give a fairly accurate representation of the size distribution for material over about 5 μm but again do not "see" all the clay (Figure 1).

We have used the Sedigraph in this work because it gives the whole size spectrum with satisfactory resolution above 1 μm [*Jones et al.*, 1988; *Coakley & Syvitski*, 1991]. Although several instruments give output as cumulative curves, we prefer to differentiate these to obtain the frequency curves, (n.b., a cumulative curve on log-log axes can conceal most significant aspects of grain-size data). One method of analyzing components is to dissect the frequency curve into its component distributions and to see whether they have distinctive composition or other properties [*Oser*, 1972; *van Andel*, 1973]. Modern computer programs [e.g., *Sheridan et al.*, 1987; PeakFit, 1990] allow this to be done interactively.

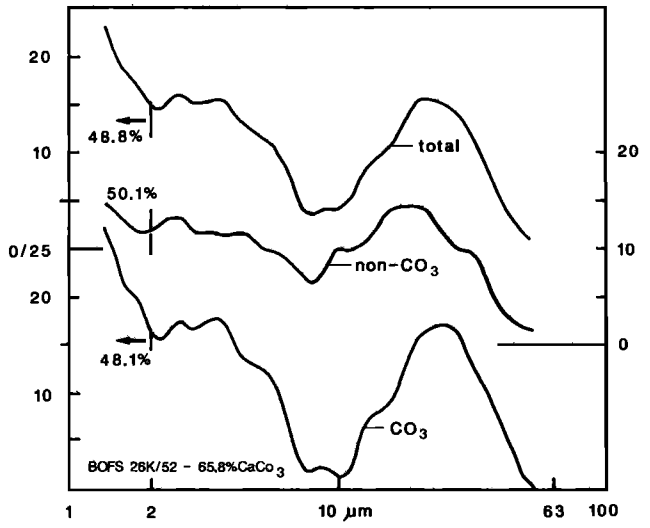

Figure 2. Size frequency distributions of components of a sample containing 65.8% $CaCO_3$. (top) Total sediment, (middle) noncarbonate fraction, (bottom) carbonate fraction. Each of the component size distributions is rescaled to 100% of the fraction. On each curve the percentage less than 2 μm is indicated. Vertical axis is frequency in percent per ϕ unit.

Size Distributions of Components

The size distribution of compositionally distinct parts of the sediment can be obtained by determining the size distribution of the sediment before and after removal of the component and determination of its amount. The most obvious one is carbonate. Simply, the total fine fraction is size analyzed, carbonate is removed gently if clays are to be analyzed later (e.g., by sodium acetate or EDTA), and the amount of carbonate C (where $1>C>0$) is determined on a subsample. The size distribution of the residue is then determined. The size distribution of the carbonate is given by the difference between the size distribution of the total minus (1-C) times the size distribution of the residue (Figure 2). Formally, in unit mass of sediment, defining the size distribution function $f(d_p)$ as $f(d_p) = dm/dd_p$, where dm is the mass of particles between size d_p and $(d_p + dd_p)$, then,

$$f(d_p)_C = f(d_p)_T - (1\text{-}C)f(d_p)_R$$

where the subscripts C, T and R denote the carbonate fraction, total sediment and noncarbonate residue, $T=(C+R)=1$. Figure 3 gives the analytical flow chart for the operations required to generate these data.

The Inference of Current Speed from Particle Size

Many size analyses of contourites made with different instruments on samples from several places show a minimum in the size distribution between about 8 and 10 μm [*Driscoll et al.*, 1985; *McCave*, 1985; *Wang and McCave*, 1990; *Massé*, 1993]. We will review the erosional and depositional behavior of fine sediments and the nature of deep-sea currents to examine the possible significance of this size break and determine what parameters for palaeocurrent inference have a good experimental and theoretical basis.

Sorting

Sediment sorting occurs principally during resuspension or deposition by processes of aggregate breakup and particle selection according to settling velocity and stress. Sorting takes place through differing rates of sediment transport, so that an originally unsorted mixture is converted downstream into narrower distributions; residue that is scarcely moved at all, and successive mixtures dominated by transport as bed load and then as suspended load. There is a substantial region of overlap between these populations. The controlling variables are the critical erosion stress (τ_e) which enters into many formulations of bed-load sediment transport rate, the critical suspension stress (τ_s) which, contrary to the supposition of *McCave and Swift* [1976] and *McCave*

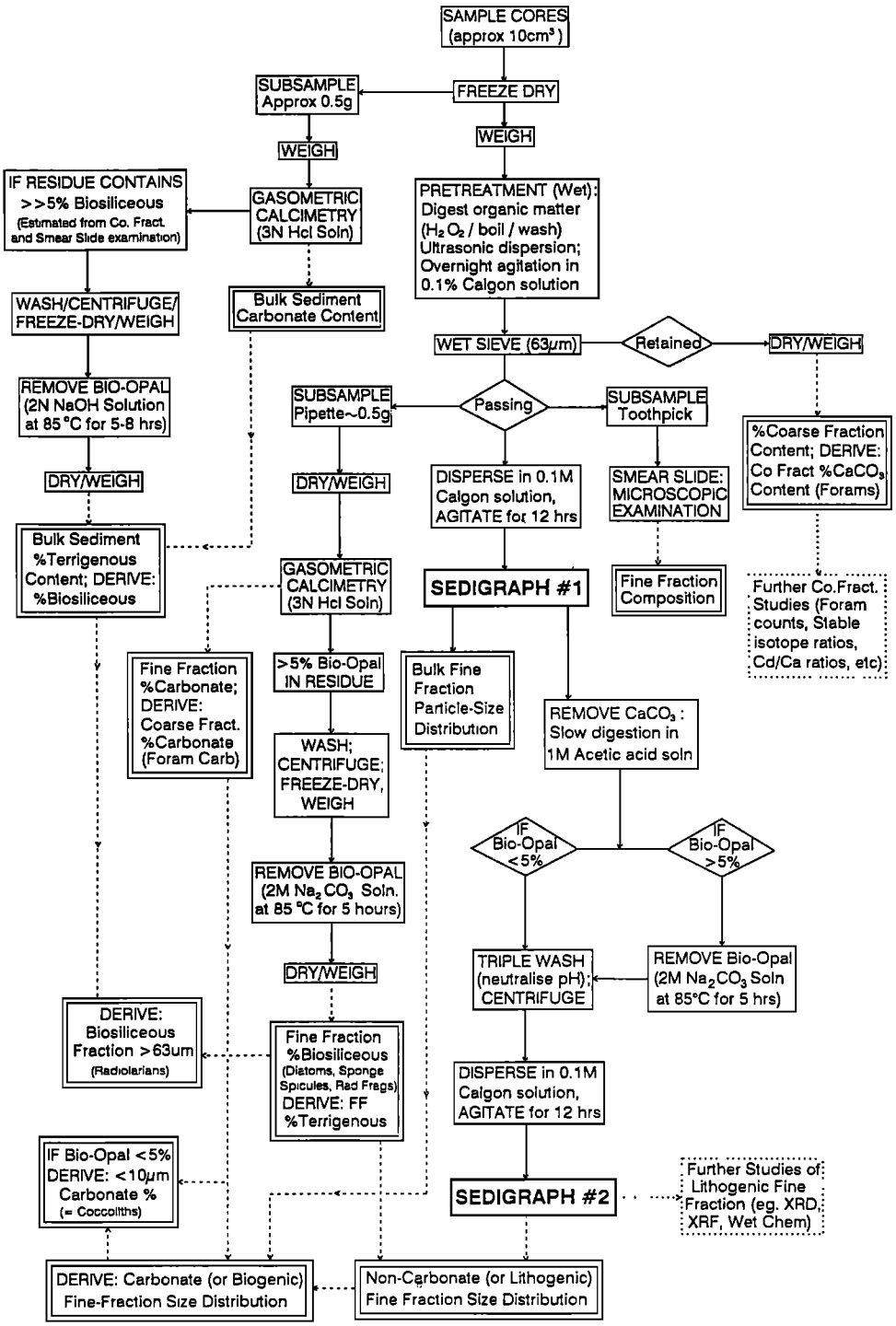

Figure 3. Analytical flow chart for size/composition slicing.

[1984], may be greater than the erosion stress for fine noncohesive silts, according to *Dade et al.* [1992], and the critical deposition stress (τ_d). In general, $\tau_d < \tau_e < \tau_s$ for noncohesive material. In the transport region between τ_e and τ_s, particle motion will be as bedload [*Dade et al.*, 1992]. Grain-bed contact bedforms and associated bedload sorting mechanisms will occur. The bedforms comprise various types of silty ripples [*Rees*, 1968; *Mantz*, 1978; *Hollister and McCave*, 1984]. The suspension that occurs as a result of bedform and biogenic roughness however will narrow this bedload region. During deposition some grains and aggregates are sorted by being trapped in the viscous sublayer, while others of smaller settling velocity w_s, in general of

$w_s < 0.64\,u_*$ [*Allen*, 1971], where u_* is the shear velocity, are not, and are transported further downcurrent.

Critical Erosion Conditions

Well-sorted fine sediments behave in a non-cohesive manner down to about 10 μm diameter. Below this size, particles start to become cohesive partly because clay minerals, with their charge imbalances, enter the compositional spectrum [Weaver, 1989 p. 10; *McCave*, 1985, Figure 20]. Also, below this order of size, van der Waals forces become significant in particle adhesion [*Russel*, 1980]. For equal sized quartz particles at 50-nm separation, the ratio of van der Waals attraction to particle weight is 0.2 for 10 μm,and 20 for 1 μm diameter. A 50-nm separation takes into account real rough particle behavior rather than ideal sphere behaviour for which 5nm would be more appropriate [*James and Williams*, 1982; *Dade and Nowell*, 1991]. The critical erosion behavior of quartz in seawater shows that cohesion starts to dominate for sizes less than about 10 μm [*Unsold*, 1982] (Figure 4). Silt flakes of >10 μm have a threshold shear velocity below that of equant grains of similar size, regardless of whether a linear dimension or a volume equivalent diameter is used [*Mantz*, 1977]. The view developed by *Krone* [1962] and *Partheniades* [1965] of the erosion process for cohesive material recognises the bed as being made up of aggregates, and erosion as involving their rupture. The sea bed generally has a loose layer of material produced by biological action, weakly bound to the substrate. The field erosion threshold data of *Drake and Caccione* [1986] from the northern Californian shelf fall within and just above the noncohesive envelope defined by *Miller et al.* [1977] (Figure 4). These sediments have a mean size of 18 μm, a pronounced mode at 25 μm, and contain ~15% clay. The authors conclude that the Shields noncohesive threshold erosion curve applies to natural clayey silts. We believe these different lines of evidence converge, showing that below about 10-μm cohesion starts to play a significant role, and that coarser sized particles will experience sorting during pickup, dependant on primary particle size.

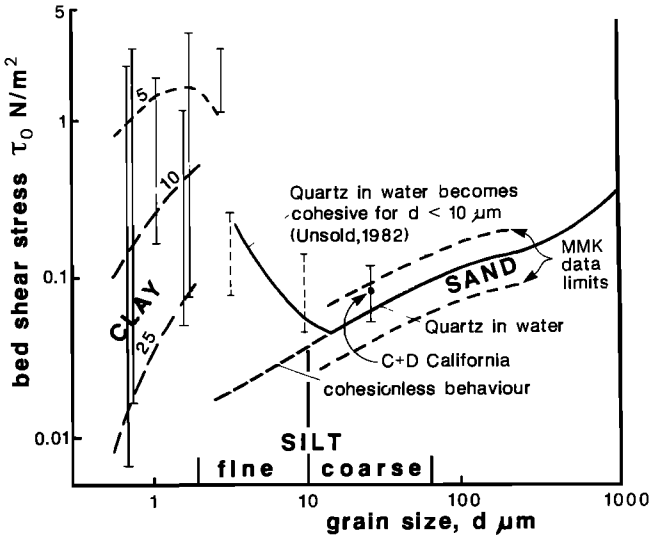

Figure 4. Critical bed shear stress τ_0 for erosion of quartz showing the onset of a cohesion effect at about 10 μm, after *Unsold* [1982]. The data in the clay range were taken from various authors and contoured for voids ratio. "MMK data limits" refers to the limits of available high-quality data evaluated by *Miller et al.* [1977]. "C + D California" is the mean and range of in situ critical erosion stress for clayey silt measured by *Caccione and Drake* [1986].

Critical Deposition Conditions

Measurements of critical deposition stress by *Self et al.* [1989] give the approximate relation $\tau_d \approx 10^3 d$ (in SI units), thus deposition of 10-μm particles occurs at stresses <0.010 Pa (shear velocity u_* <0.32cm s^{-1}). These values, obtained in a radial laminar flow cell, are rather less than the critical deposition stresses taken by *McCave and Swift* [1976] to be approximately equal to erosion stress of particles with the same settling velocity, and which yield ~0.045 Pa (u_* = 0.67 cm s^{-1}) for 10-μm silt, or 0.015 to 0.03 Pa via the analytical expression of *Dade et al.* [1992]. The trend of these curves, however is the same. This range of shear stresses (0.01-0.045 Pa) is a little lower than that indicated by *Hunt*'s [1986] experiments for the breakup of montmorillonite and illite flocs due to shear, namely 0.04 to 0.16 Pa. For shear stresses less than the critical breakup value, aggregates are likely to remain intact in the high shear region of the viscous sublayer, but at higher values they are likely to be broken up, and deposition will occur as primary particles. The implication is that most aggregates less than about 10 μm in diameter will survive during deposition from currents, but above that size they are increasingly likely to be disaggregated in the viscous sublayer. Hydrodynamic processes of sorting in the viscous sublayer will thus tend to act on primary particles for sizes greater than 10 μm. There is also some primary deposition of much larger aggregates (marine snow) on the seafloor. These are subject to degradation and, in current-swept areas, resuspension and deposition of their surviving components [*Lampitt*, 1985].

Thus both erosional and depositional considerations indicate that primary disaggregated particle sizes should be related to the fluid shear environment when the particles are larger than about 10-μm. The data are not so precise as to specify 10 μm exactly, and the region 8 μm (=7 phi) to 11 μm (6.5 phi) may be considered a transition region for this behaviour, but for the sake of

definiteness (and other anthropomorphic reasons) we will use 10 μm.

Size Distributions Under Modern Ocean Currents

Sediments from the continental margins of the eastern United States, Nova Scotian Rise, and Argentine Basin have been examined by *Bulfinch and Ledbetter* [1984], *Driscoll* et al. [1985] and *Ledbetter and Klaus* [1987]. In the cases of the eastern United States and Argentine Basin, the noncarbonate silt-mean size approach of Ledbetter shows a general relationship between coarser silt mean and the path of deep western boundary currents as defined by turbidity [*Eittreim et al.*, 1976] and hydrography [*Georgi*, 1981; *Weatherly and Kelley*, 1985]. The available data, however, do not allow a relationship to be derived between silt mean size and long-term mean current velocity. Indeed, simply using mean scalar speed would not be appropriate and mean velocity even less so. Some measure of the effectiveness of competent currents, those with flow speeds yielding a critical erosion shear velocity $u_{*c} \geq 0.7$ cm s^{-1} (equivalent to geostrophic velocity over 15 to 21 cm s^{-1}, [*Weatherly*, 1984]), would need to be extracted from records of current meters set at 50 to 100 m above the bed. Such a measure might be $(u_* - u_{*c})^3 t$ for $u_* > u_{*c}$, where t is the fraction of a year that a given u_* acts.

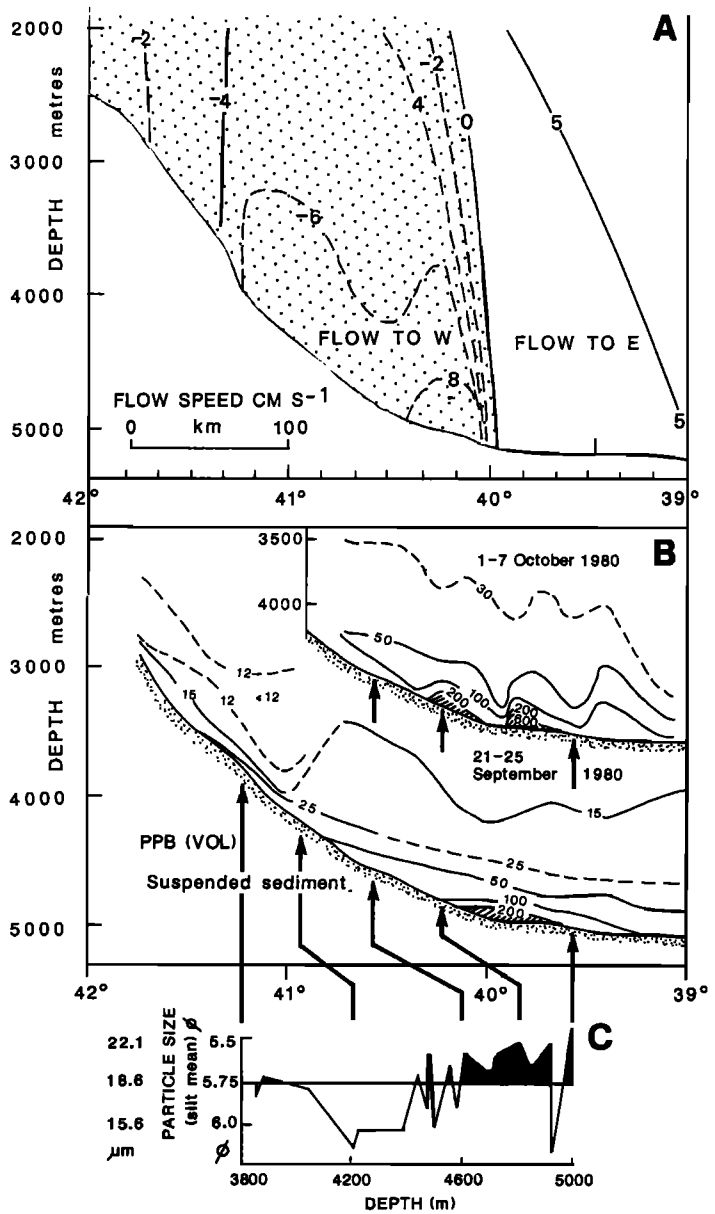

Figure 5. Distribution of (a) measured mean current velocity [*Hogg et al.*, 1986], (b) suspended sediment concentration ppb by volume [*McCave*, 1983] and (c) silt mean size [*Bulfinch and Ledbetter*, 1984] across the Nova Scotian Rise between 60° and 65°W.

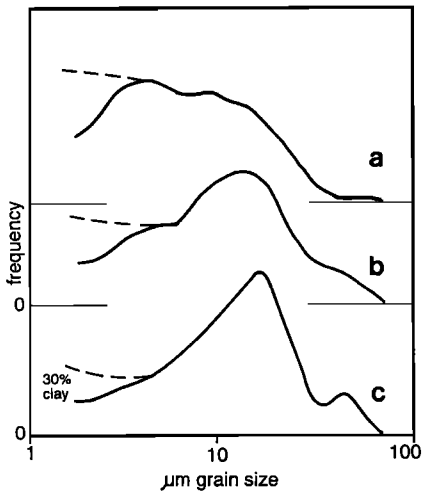

Figure 6. Size distributions of sediment from the Nova Scotian Rise measured by Coulter Counter [*McCave*, 1985], showing (a) dominance of a 4-μm mode and a weak 10-μmmode under slow currents at 4000 m water depth, (b) bimodal structure at 4800 m deposited after moderate currents of 5-10 cm/s, and (c) well developed 16-μm mode at 4800m deposited after strong currents (10-15 cm/s).

The data for the Nova Scotian Rise were obtained both by Elzone counter and expressed as silt mean size [*Bulfinch and Ledbetter*, 1984] and by classical pipette method displayed as frequency curves [*Driscoll et al.*, 1985]. The curves were clearly bimodal with a coarse silt mode at about 16 μm and a clay mode below 2 μm. The height of the ~16-μm mode and the silt mean size increased towards the lower part of the rise where turbidity, hydrographic and current meter data indicate stronger currents [*Weatherly and Kelley*, 1982, 1985; *McCave*, 1983; *Richardson et al.*, 1981; *Hogg et al.*, 1986; *Ezer and Weatherly*, 1991] (Figure 5). Detailed analyses by Coulter Counter at the HEBBLE site on the Nova Scotian Rise showed a bimodal size structure in the window 1.6 μm to 80 μm with modes at 3-4 μm and 12-17 μm (Figure 6) [*McCave*, 1985]. The 3-4 μm fine silt mode is positively correlated with percentage of clay and is thought to be an instrumentally truncated remnant of the main clay peak below 2 μm. The coarse mode is inversely correlated with % clay (Figure 7). This indicates the size-sorted behavior of the silt coarser than about 10 μm in diameter, versus the unsorted cohesive behavior of the fine silt and clay, and lends credence to the notion of sortable, noncohesive behavior of the coarse silt fraction. However, we cannot yet obtain a quantitative relationship between sedimentary parameters and measured current speeds. Nevertheless, the range of measured eroding and depositing velocities on the Nova Scotian Rise is consistent with applicability of the laboratory erosion and deposition stresses (Figure 4). (Geostrophic velocities are related to shear velocity by $U_g = 30u_*$ to $22u_*$ depending on drag coefficient [*Weatherly*, 1984]). Thus experimental data indicate a critical erosion shear velocity of ≈0.70 cm/s for 16 μm silt, which is close to the 0.68 cm/s deduced for the HEBBLE site by *McCave* [1988] from the data of *Gross and Williams* [1988], and is produced by U_g of 15 to 20 cm s^{-1}. The coarse silt size parameters record the effectiveness (duration x work rate) of currents faster than this.

Nature of the Currents That Sort Deep-Sea Sediment

We must now enquire about the dynamical origin of the currents responsible for resuspension of sediments, for without resuspension there will be little sorting. We need to know this so that we may have a secure basis for interpretation of the properties of sorted sediments. Several idealized cases of current time series may be imagined (Figure 8). In Figure 8a the flow speed is constantly above critical for a certain size, resulting in erosion of that material and a residue of coarser sediment. A current that never reaches critical (Figure 8b)

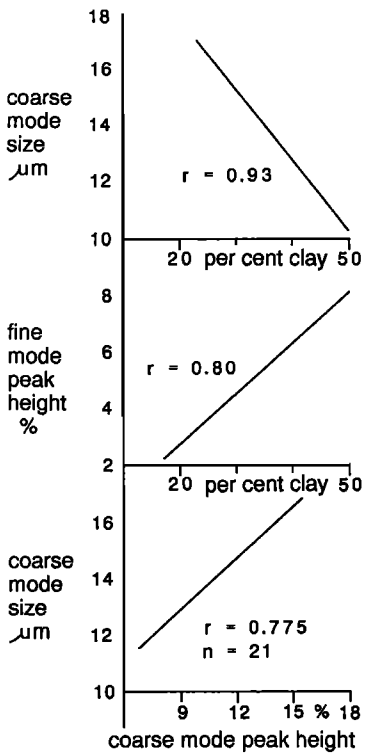

Figure 7. Correlations between parameters of size distributions from the Nova Scotian Rise showing sorting in the silt range (see Figure 5b for meaning of fine and coarse modes). (a) coarse silt mode is coarser with less clay, (b) there is more fine silt mode with more clay, (c) coarse mode size and peak height are positively related. Figure is after *McCave* [1985].

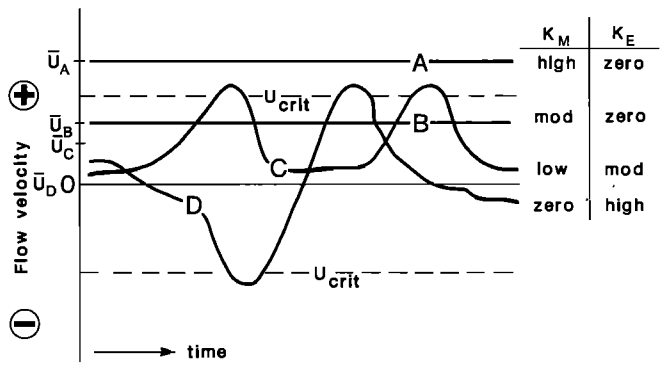

Figure 8. Idealized time series of currents. The time axis could represent a scale of days or months.

will produce no effect, even though it has a faster mean than a variable current (Figure 8c) which occasionally exceeds critical. This is the common case of a current with an underlying mean and an added source of variability. Finally, Figure 8d represents the situation of zero (or very small) mean current and large variability such that currents in several directions are able to move sediment but with zero net transport. The important cases are clearly shown in Figures 8c and 8d. The key question is whether the inference to be drawn from a change in sorted sediment is of a change in the underlying flow (mean kinetic energy K_M) or a change in the variability (eddy kinetic energy K_E).

The origins of the mean flow are mainly deep geostrophic currents driven by temperature and salinity differences [*Pond and Pickard*, 1983; *Warren*, 1981]. There is also a strong influence of the magnitude of the slope along which geostrophic currents flow. A steeper bed slope supports a locally steeper isopycnal gradient and faster current, [*Bowden*, 1960; *McCave*, 1982]. Thus on steep scarps very fast currents are inferred geostrophically and measured by current meters [e.g., *Warren*, 1973; *Bird et al.*, 1982]. In some regions of significant eddy activity a deep mean flow may be driven by eddies [*Holland and Rhines*, 1980], and *Hogg et al.* [1986] suggest that the deep flow over the Nova Scotian Rise is driven in this way. There is embedded within this eddy-driven flow a deep western boundary current (DWBC) of Norwegian Sea Overflow Water and a deeper cold filament of Antarctic Bottom Water [*Weatherly and Kelley*, 1985]. Thus, even the mean flow of a DWBC, in special settings, may not be entirely due to geostrophy. The setting on the Nova Scotian Rise is just to the north of the mean position of the Gulf Stream and under the path of warm-core rings shed from it. The idealized time series of Figure 8d is thus rather unrealistic in that regions of high eddy energy are likely to have a mean flow driven by eddies. The Argentine Basin may well be a place where the eddy and mean-flow energy both contribute to sediment sorting, but their relative contributions cannot be identified. The net size trend of *Ledbetter and Klaus* [1987] certainly follows the residual flow.

Tidal and inertial motions are averaged out prior to estimation of deviations from the mean in calculating K_E. However there are settings where the internal tide is of significant magnitude and provides the necessary addition to the mean to push the speed beyond critical erosion conditions (Figure 8), (the direct baroclinic tidal current due to sea surface slope is small, 1 or 2 cm s^{-1} at most). The internal tide is intensified in regions where the local bottom slope (α) matches that of the characteristic. This is most simply given by $\sigma^2 = N^2 \sin^2\alpha + f^2 \cos^2\alpha$ [*Thorpe and White*, 1988], in which the frequencies are σ for the internal tide, f for inertia (Coriolis) and N for buoyancy, given by $N^2 = (g/\rho)(\partial\sigma_t/\partial z)$, where ρ is the in situ density and σ_t the usual density parameter. The key variables are the bottom slope and the potential density gradient. Work on Porcupine Bank has shown internal tidal control of resuspension at two depths [*Dickson and McCave*, 1986; *Thorpe and White*, 1988]. At the deep levels (1800-2800 m), currents near the bed exceed 15 cm s^{-1} for 1.8 to 4.1% of the time [*Thorpe*, 1987]. The tidal cases illustrated in Figure 9 are from regions with sedimentary features of current origin; foraminiferal sand dunes at the foot of Hatton Drift (Figure 9a); mud waves on top of Hatton Drift (Figure 9b); and furrows on the Saharan Rise (Figure 9c). At the sand dune site the flow exceeds 15 cm s^{-1} most of the time and is expected to be erosional (for silt), whereas the flow on top of Hatton Drift is, in this very short record, always subcritical for erosion but has sufficient stress to result in sorting during deposition.

In recent years the pronounced effects of eddy energy on the sea bed have been recognized as "benthic storms" [*Hollister and McCave*, 1984; *Gross and Williams*, 1991]. In these, long-period variability of the deep flow shows short episodes of intense sediment resuspension (Figure 9d). Storms have been examined in any detail only on the Nova Scotian Rise where they are westward directed bursts of energy resulting from Rossby wave-like motions which are probably forced by the Gulf Stream [*Welsh et al.*, 1991]. The motions are coherent throughout the water column from top to bottom, a feature also seen in the eddies near the Kuroshio Extension, where the abyssal K_E is about 100 cm^2 s^{-2} less than beneath the Gulf Stream [*Schmitz*, 1984a, b]. This vertical coherence means that regions of high abyssal K_E underlie high surface K_E which is mapped by satellites using variability of sea surface elevation [*Zlotnicki et al.*, 1989] or slope [*Sandwell and Zhang*, 1989; *Shum et al.*, 1990].

Purely on the basis of sedimentary properties we cannot distinguish whether a change in size is due to an increase in the mean speed or an increase in the variability of speed. On the other hand, one can identify

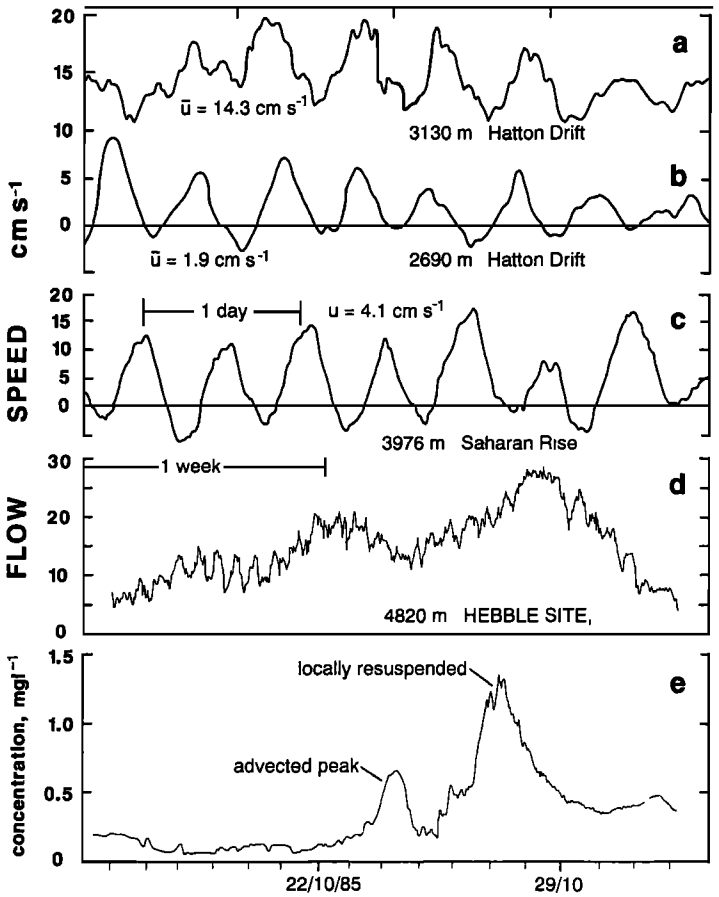

Figure 9. Time series of deep ocean currents measured near bed. Internal tides on (a) a strong mean flow and (b) a weak mean flow (both on Hatton Drift from *McCave et al.* [1980]), (c) a moderate mean flow over a furrowed bed [*Lonsdale*, 1982], (d) two and a half weeks record of a storm at the HEBBLE site on the Nova Scotian Rise with (e) turbidity record showing main storm on 27 October. Note tidal signal also present in Figure 9d, from *Gross and Williams* [1991].

those oceanic regions where strong mean flow and those where strong eddy variability is likely to occur [*Dickson*, 1983]. In some regions both signals are found and these will present difficulties in interpretation of sediment. Clearly, an important strategy for the inference of flow speeds bearing on palaeocirculation is to sample regions where the eddy K_E is likely to have been low and mean K_M relatively high. Places to avoid are the North American Basin north of about 30°N, the Argentine Basin, the North Pacific near the Kuroshio, the Agulhas off South Africa and most of the Antarctic Circumpolar Current [*Shum et al.*, 1990]. This should hold good for the Pliocene and Pleistocene where meridional plate displacements are not more than a few hundred kilometers, but for earlier times, difficulties will be encountered.

Current Related Sediment Parameters

The best current-related parameters are probably modal or mean size of the 10-63 μm fraction. *McCave* [1985] shows that there is a good relationship between modal size and peak height so either would do, but size would be preferable as it is related to flow speed experimentally. These are both rather sensitive to analytical method, so we have selected the mean size of the 10-63 μm fraction which is more robust. Ledbetter's 4-63 μm silt mean includes part of the spectrum which is sensitive to current sorting and part which is not (Figure 7). *Ledbetter* [1986] shows that the mean responds positively to measured currents in Vema Channel. We think it wise to cut out the 4-10 μm part of the size spectrum which tends to make the parameter less precisely responsive because it behaves in the opposite way to the 10-63 μm fraction (Figures 7a and 7b). Note that Ledbetter's [1986] Figure 2 gives $U = 183.4 - 30\phi$, relating mean speed in centimeters per second to ϕ size, a relationship with a much steeper slope than that expected from a graph of critical conditions [*Miller et al.*, 1977], which is $U = 48 - 4.5\phi$.

If the deposition rate of finer material (< 10 μm) is

diminished under faster currents, because, on average, finer particles are found in aggregates of lower settling velocity [*Migniot*, 1968], and larger faster settling aggregates which might otherwise be deposited are weaker and tend to break up, then one would expect the ratio of 10-63 μm material to total fine fraction to increase with current speed. A useful index could thus be a percentage-based enrichment factor using the ratio of 10-63μm material to the total fine fraction. This index is very dependant on location in relation to sediment focusing (e.g., on a slope or at the bottom of a slope). Deeper areas or depressions simply tend to receive more fines winnowed from areas higher up, due to gravitational settling. Two areas may have similar current speeds and this will be reflected in similar trends in coarse silt mean, but each will have a different percentage of fine silt and clay dependant on its topographic setting. Nevertheless, if one wishes to compare time-trends at a single point where the topography has remained fairly constant over the sampled period, the percent >10 μm is useful. It does not behave in exactly the same way as the coarse silt size as the long time series of Figure 10 shows. The amplitude of the coarse silt size and percentage >10 μm is strongly coherent at the major orbital frequencies, but the percentage peak leads (occurs before) the size peak by about 17 ka at the 125 ka period and 1.7 ka at the precession periods. The part of the record illustrated (1.2 to 0.85 Ma) is dominated by precession and tilt forcing, for which the temporal lags are not important, but we cannot explain the 17 ka lag in the eccentricity band, unless it is related to a precession effect.

With compositional slicing a percentage based index can be made for terrigenous and carbonate material combined [*Robinson and McCave*, 1994]. This gives a way of eliminating competing influences on sediment texture, namely to record the common variance of the size of the carbonate and terrigenous fractions. It was suggested by *Wang and McCave* [1990] that only currents can act to produce more or less similar effects on the >10 μm biogenic and lithogenic fractions (Figure 11). The interglacial samples from Hatton Drift show a clear

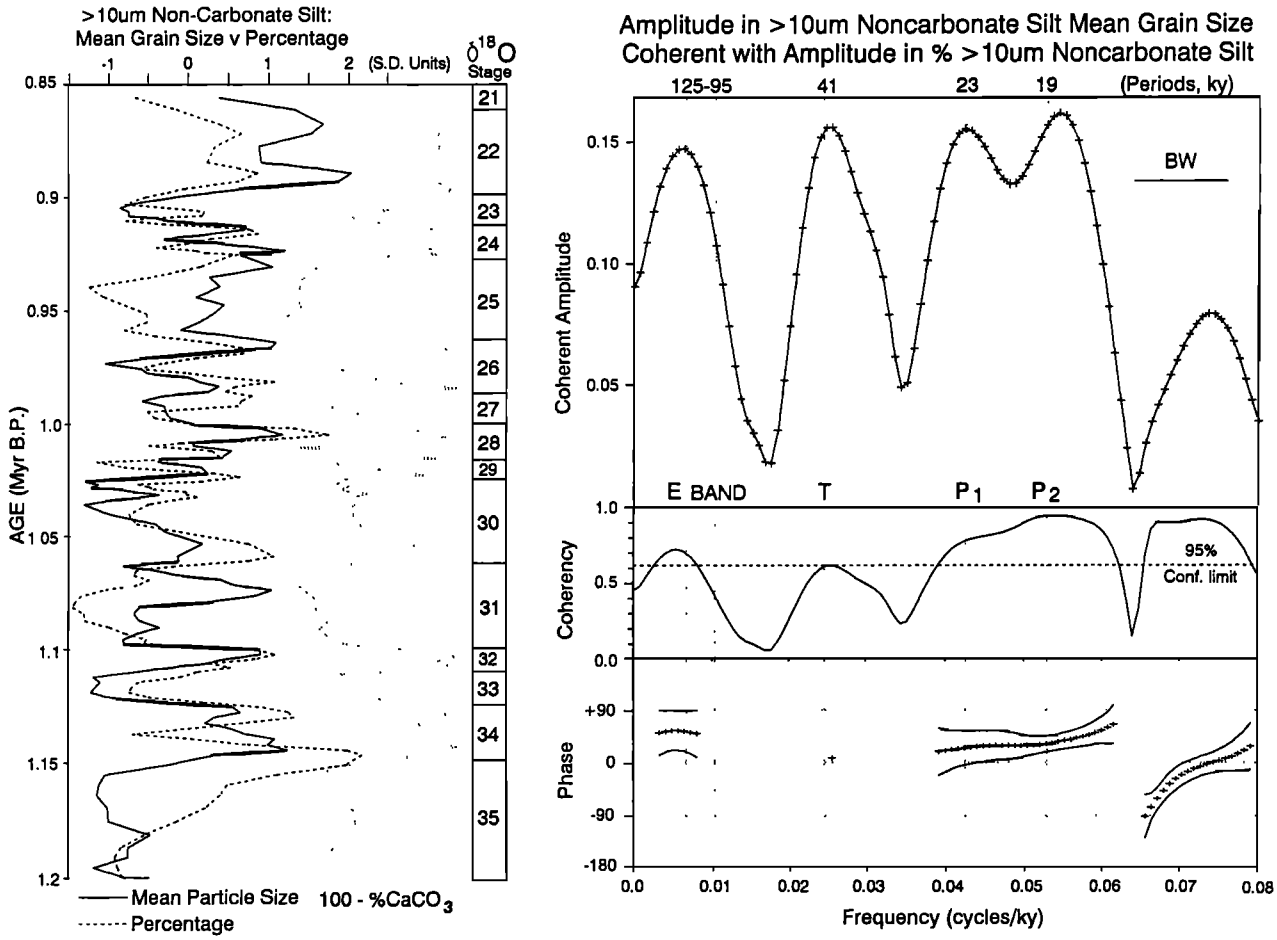

Figure 10. (left) Time series of coarse silt mean size and percentage expressed in variance units, and (right) frequency spectrum of the coherent amplitude of the two time series (DSDP Site 610A, Feni Drift).

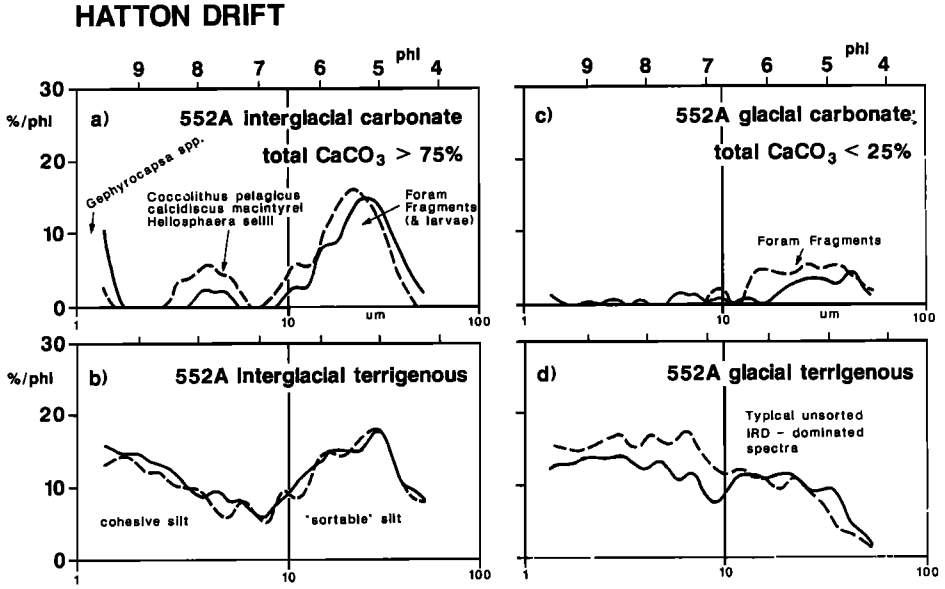

Figure 11. Average size distributions of interglacial and glacial samples for carbonate and terrigenous components from DSDP Site 552A on Hatton Drift from *Wang and McCave* [1990]. Note the pronounced >10-μm mode in both interglacial components, coccolith size peaks, and lack of these in the glacial samples. Solid and dashed lines distinguish sets of four-sample averages from glacial and interglacial periods.

correspondence of both a size mode and enrichment of the coarse terrigenous and carbonate silt relative to those from the glacial (Figure 11). The mass accumulation flux of 10-63 μm carbonate and terrigenous sediment can also be derived, given an age model, but it is not obvious whether this should increase or decrease with increasing current speed, probably decrease.

An Aside: Wind Speed-Related Sediment Parameters

Parkin [1974] formulated an atmospheric dust winnowing model in which particles finer than 7 μm are scavenged by rain with no size dependence (i.e., an aggregation process of particles with raindrops), whereas larger sizes fall out by gravitational settling depending on d^2. This size limit is comparable with the 10 μm chosen here for single particle deposition under water. Parkin related the slope of the cumulative weight percentage size distribution to the wind "vigour" Uz in which z is the height to which the dust is initially mixed in the atmosphere and U is the mean migration velocity of the depositing air mass across the sea. This gave plausible estimates of glacial winds off West Africa.

Provenance

Corliss et al. [1986] made the unsupported assertion that there will be an influence of changing sediment provenance through the glacial-interglacial cycle which affects the inference of water mass velocities from sediment size. There are several modes of sediment delivery which may vary on glacial to interglacial and other time scales. We must focus on the delivery of sediments to depths at which the deep circulation affects them. This delivery is largely by gravitational processes (turbidity currents and debris flows) but also via wind and shelf edge and slope resuspension by internal tides with subsequent rain-out from intermediate nepheloid layers. It is often assumed that turbidity currents are more frequent at low stands of sea level, yet the available data suggest all of the following; triggering at times of sea level change, triggering by 23 ka climatic changes, and uniform high-frequency from glacial to Holocene [*Weaver et al.*, 1992; *Weltje and de Boer*, 1993; *Schönfeld and Kudrass*, 1991]. The mass failures yielding large turbidity currents and debris flows involve failure of ten to several tens of meters of sediment on the slope [*Embley and Jacobi*, 1977], thereby mixing the products of several glacial-interglacial cycles [*Weaver and Thomson*, 1993]. Basal erosion by turbidity-currents will also produce a mixture, and it is hard to see how any resedimentation mechanism can deliver a pure glacial or interglacial signature.

Fluvial delivery direct to the mid-late Pleistocene shelf edge occurs only at the minima of sea level (120 to 130 m lowering, e.g. in stage 2, part of stage 6, etc.) which represent only a small proportion of the whole glacial period [*Shackleton*, 1987]. For the rest of the time, sea level lowering of less than ~90 m puts the shoreline some way back from the edge on the middle

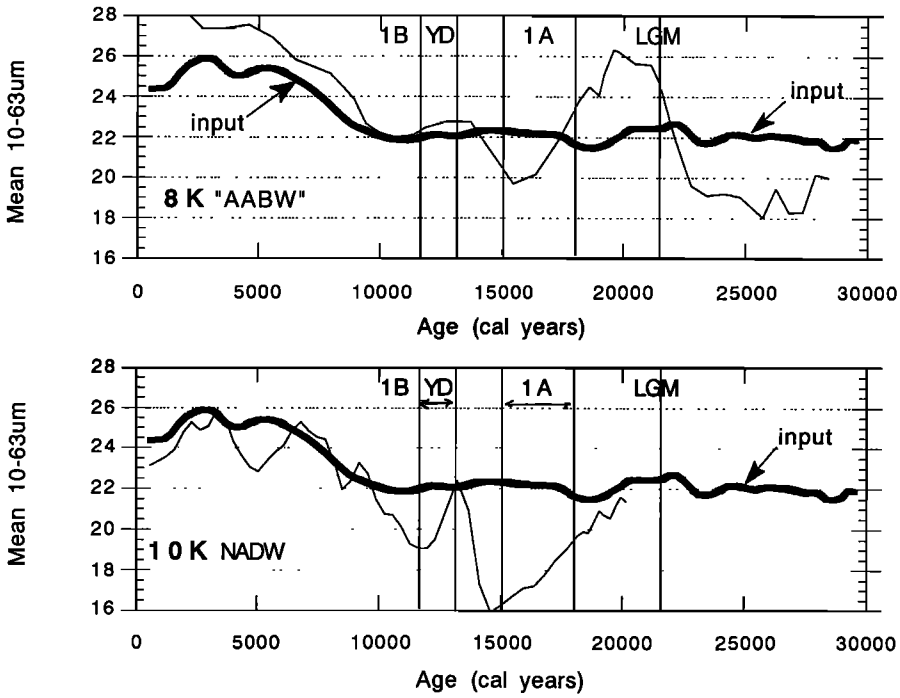

Figure 12. Change in the coarse silt mean size at two current-affected sites in the NE Atlantic compared with the size of the input function from a nearby pelagic site relatively unaffected by currents. The time scale is in calender years and the times of the last glacial maximum, terminations IA and IB and the Younger Dryas are shown for reference [after *Manighetti and McCave*, this issue).

of the shelf. The point is that material is delivered to the deep sea via resuspension processes, not direct delivery, most of the time. The sea level minima do result in some rapid supply of continental detritus to the deep-sea circulation, as demonstrated by maxima in red/pink coloration of sediments beneath the Western Boundary Undercurrent originating from Upper Palaeozoic redbeds of the Canadian Maritime Provinces, during glacial stages [*Hollister and Heezen*, 1972]. On glaciated margins direct delivery by ice occurs to the top of the slope, and from ice rafting to the slope and deep sea beyond [*Fillon*, 1985; *Boulton*, 1990]. Ice-rafting increases North Atlantic sedimentation rates from about 2 cm/ka [*Balsom & McCoy*, 1987] to 3 to 4 cm/ka at most on average [*Manighetti & McCave*, this issue], much less than the enhancement that can occur under deep current systems on sediment drifts (up to 25 cm/ka). There are brief periods of very rapid ice-rafted desposition (Heinrich layers) in which direct delivery dominates [*Bond et al.*, 1992]. Sampling schemes need to recognize the existence of such layers for sedimentological and stratigraphic analysis.

It is not obvious that these processes would deliver a coarser mixture in the coarse silt range during glacials. A coarse base to turbidite units would be expected, but the currents start off by eroding the fine top of earlier turbidites. Winds do appear to deliver a coarser mixture in the glacials, at least in the trade wind belt [*Parkin*, 1974]. There is no clear reason for supposing that wind-wave erosion of the outer shelf at low sea level stand will yield a suspension with a coarser silt (>10 μm) mean than internal wave erosion at high sea level stand. The input function of *Manighetti and McCave* [this issue], spanning the last 30 ka of pelagic (including ice rafted) deposition on the East Thulean Rise shows an increase in the coarse silt mean size of about 3 μm in the last 7 ka (Figure 12). Although the mass flux may be greater in the glacial, the material does not have a coarser silt size. We would not wish to generalize from this profile to other regions, but argue that there is no a priori reason why the sediment available to be transported by deep-sea currents should show systematic short-term shifts on timescales of 100 ka or less which might be confused with a current-controlled origin. On much longer timescales, major tectonic and climatic changes will influence differences in delivered size through changes in mountain elevation and stream gradient and weathering style and intensity.

Size-Composition Slicing

The earlier section on inference of size distributions of components means that we can now subdivide the terrigenous and carbonate fractions. That is to say we

Table 1. Size Differentiated Components of Deep-Sea Sediments

	Fine Fraction			Coarse Fraction
	Clay,	Silt		Sand,
Composition	<2 μm	2-10 μm	10-63 μm	>63 μm
Lithogenic	clay minerals Fe/Mn oxides/ hydroxides	quartz, feldspar, mica, clay minerals	quartz, feldspar, mica, glass shards	rock fragments (IRD) quartz, feldspar, glass shards, pumice
Biogenic Carbonate	small coccoliths (*Gephyrocapsa spp*), coccolith fragments	coccoliths (except *Gephyrocapsa spp.*)	foram.fragments (and larvae)	foraminifera, detrital carbonate (IRD)
Silica	diatom fragments	sponge spicules diatom fragments	diatoms, radiolarian fragments	radiolaria

can determine the proportions and size characteristics of different parts of the spectrum. The significance of a 10-μm boundary has been urged in relation to the terrigenous fraction. This size is also a useful boundary in carbonate sediments, because very few Pleistocene coccoliths have a settling velocity (Stokesian) equivalent size greater than 10 μm [*Okada and McIntyre*, 1977]. Above the lysocline, carbonate <10 μm is dominantly coccoliths. Below the lysocline there may also be a component of very small foram fragments. In North Atlantic Heinrich layers there is an appreciable amount of fine Palaeozic carbonate and Cretaceous chalk, so vigilance is required. In theory the component subtraction method could yield the size distribution of carbonate, opal, and terrigenous fractions. However the compounded errors of size and component determination mean that it is not possible to determine reliably the size distribution of a component of less than 10% of the whole. Most of the sediments we have dealt with do not have sufficient opal to make the effort worthwhile.

Adoption of a 10 μm boundary allows us to pick four size ranges for material using commonly accepted classes (<2, 2-10, 10-63, >63μm), that is clay, fine silt, coarse silt, and sand. Within the sand fraction it is a simple matter to physically separate subsamples using sieves. These size ranges have fairly clear (though not exclusive) identities (Table 1).

An example of what can be done through recognition of components is shown in Figure 13 where two peaks in the size spectrum can be associated with different coccolith species. Figure 11 also shows two coccolith size peaks in the <10-μm fraction. Because of the overlap in the size of species it has been necessary to lump *Reticulofenestra minuta* and *Dictycoccites productus*, but it shows that some distinctions can be rapidly made via modal peak heights which otherwise would require a lot of counting. Plotting the downcore peak height ratios for Sites 552A and 610A in the upper Pliocene, *Jones* [1988] found a synchronous shift in relative species abundances which may be related to a circulation or productivity change.

Using the percentage of fine (coccolith) carbonate in conjunction with an age model permits derivation of continuous mass accumulation rates which, at a shallow site like 610 (2500 m), are related to productivity. Spectral analysis of these by *Robinson and McCave* [1994] shows very clear coherence with the model of orbitally forced ice volume fluctuations of *Shackleton et al.* [1990] at 41 and 23 ka (Figure 14). There is a very slight phase lag of 2 to 3 ka with productivity following ice volume peaks. The coccolith productivity is not strongly driven by the 100 ka glacial-interglacial cycle, and it is not always associated with warm periods of low ice volume. The 10 to 63 μm carbonate material is mainly fragments and larvae of foraminifera. In glacial sediments there is sometimes significant carbonate silt (such as in the ice-rafting pulses documented by *Andrews and Tedesco* [1992]), but normally the material consists of foram fragments. This material is also sortable, and allows derivation of a parallel current strength index (the mean size of the >10-μm carbonate silt) to go alongside that based on the terrigenous fraction. This will clearly be suspect near or below the lysocline and even above that level this size should always be considered alongside the noncarbonate silt size.

Data from coarse fraction analysis may be combined with information from the fine fraction. For example,

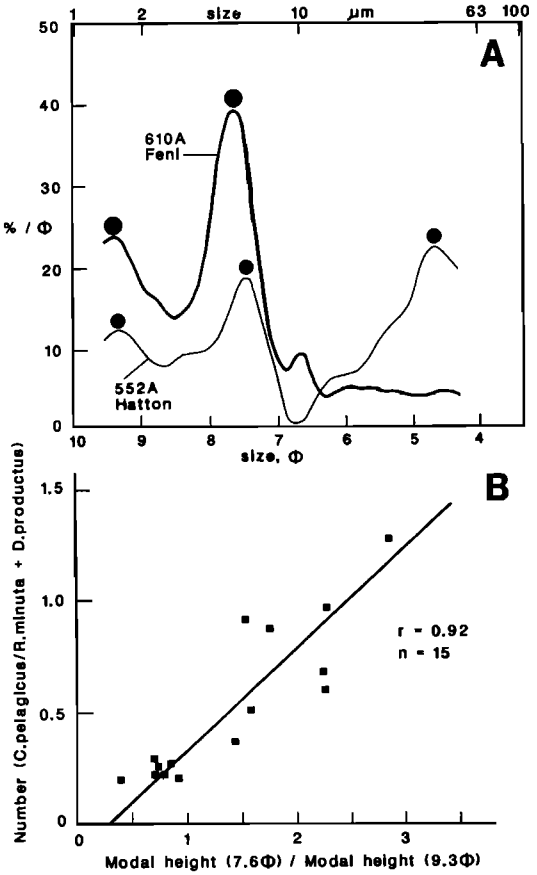

Figure 13. (a) Size distribution of Pliocene carbonate-rich (94%) sample from Feni Drift (DSDP Site 610A/17-/3/78) showing modes at 9.3ϕ (1.60 μm) and 7.4ϕ (5.9 μm) which represent *R.minuta* plus *D.productus* and *C.pelagicus* respectively. The comparable sample from Hatton Drift (DSDP Site 522A/11/1/6) also shows a strong foram fragment mode at 4.7ϕ. (b) Close relationship between modal peak height ratio and abundance ratio of species counted in smear slide [from *Jones*, 1988].

terrigenous sand is an excellent indicator of ice rafting and expressing its abundance in variance units provides a basis for subtracting ice-rafting effects from time series of silt abundance in order to try and eliminate provenance artifacts. In the same way more foram fragments are expected in the silt fraction when foram abundance is greatest, and subtraction of foram variance helps isolate current effects. This operation can be carried out on either percentages or mass accumulation rates and is illustrated for Feni Drift (DSDP Site 610) by *Robinson and McCave* [1994].

Conclusions

We conclude that fine sediment shows increasingly noncohesive behavior above 10μm and cohesive below that size. The silt coarser than 10μm responds largely as single particles to hydrodynamic forces on erosion and deposition because of the breakage of aggregates and is therefore size-sorted according to shear stress. Thus the size of the >10-μm silt is a useful current strength indicator. Because deposition of coarser material under faster currents also involves suppression of deposition of finer sediments, the percentage of >10-μm silt in the fine fraction (<63 μm) is also an indicator of current strength at a point, but variability of sediment focussing poses problems when comparing time series of percentage data from different topographic settings.

There is no good reason to believe that there are systematic short-term changes in delivered silt size related to provenance on time scales <100 ka. Mixing of sediment during turbidity current, debris flow and slope resuspension delivery to the site of deep current sorting means that systematic changes are not to be expected. For some sites far from continental margin input, definition of a pelagic input function from sites relatively unaffected by currents gives a basis for assessment of relative changes in current speed. In general the increase over general pelagic sedimentation rates caused by current-controlled focusing is much greater than that caused by ice-rafting, other than in Heinrich events.

These sediment parameters are not capable of resolving whether the currents responsible for sorting have a small mean and large variability or large mean and small variability. For inference of the flow speeds of water masses the latter situation is required. For the late Quaternary at least we suggest that the distribution of eddy kinetic energy was similar to the present (though with some latitudinal compression in the Gulf Stream area), and that places to avoid can be assessed using the products of satellite altimetry. These are the N. American Basin north of 30°, Argentine Basin, Kuroshio area, Agulhas retroflection and Antarctic Circumpolar Current. Steepening of the density gradient $\partial\sigma_T/\partial z$ can also result in local intensification of internal tidal currents, and this contributes another interpretive pitfall to be examined carefully.

The size of compositionally distinct components of a sediment can be inferred from the difference between the total size distribution and the size of the residue after a component has been removed by dissolution. This allows estimation of size parameters of carbonate separate from terrigenous material, and in principle opal if sediments contain sufficient biosiliceous material for precise determination (more than 10 to 15%). The fine carbonate is dominated by coccoliths below 10 μm and foram fragments or larvae in the fraction 10 to 63μm. The coarse carbonate silt fraction is also current sorted and, when combined with the index based on terrigenous silt, gives a more robust current speed index. Coccolith carbonate mass accumulation rate is principally related to productivity for pelagic sites above the lysocline

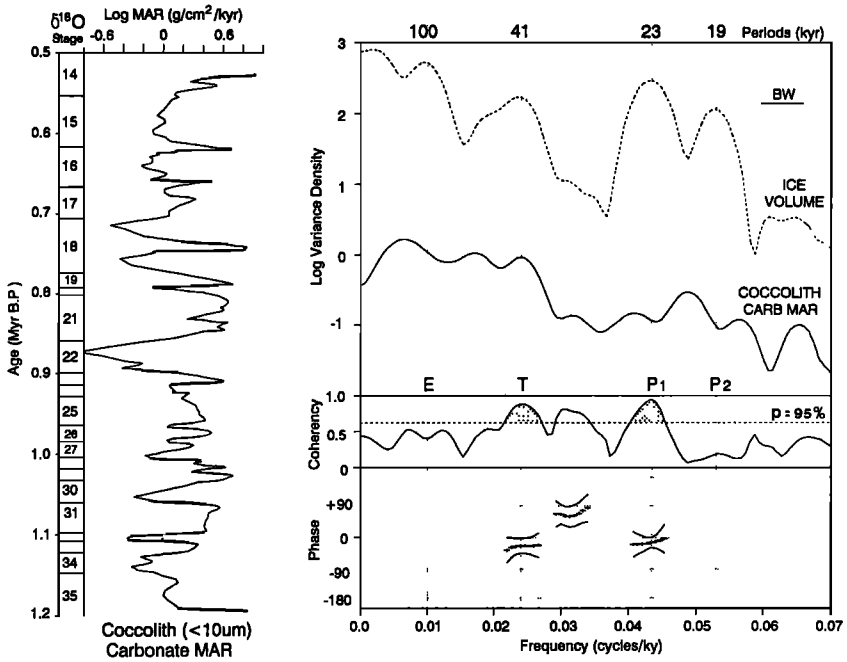

Figure 14. (left) Early to mid-Pleistocene variation in coccolith (<10 μm Ca CO_3) mass accumulation rate (log g cm^{-2} ka^{-1}) expressed in variance units of the time series. Spectrum of log MAR, ice volume model and the coherency between them. Pronounced coherency at obliquity and precession frequencies is apparent with a small phase lag [from *Robinson and McCave*, 1994] DSDP Site 610, Feni Drift.

(though clearly strong currents would render such an inference unsound).

These techniques are somewhat laborious (Figure 3), but it is possible to process 50 to 100 samples per week and thus obtain higher resolution quantitative sedimentological data than hitherto for long time series in which both current and productivity-related effects may be important.

Acknowledgments. We thank Gillian Foreman and Neil Pickard for laboratory assistance, Eric Browne, Dave Martel, and Pravin Patel for assistance in interfacing and programming the Sedigraph, Karen Jones for her work on coccolith sizes and counts, Jeremy Young and Jan Backman for advice on coccolith sizes, and Brian Dade, Mike Ledbetter and Brian Haskell for their review of the manuscript. We thank the NERC of U.K. for grants GST/02/426 (McCave, Elderfield, Shackleton, Manighetti) for BOFS, and GST/02/436 (McCave and Robinson) for DSP/ODP core work. Cambridge Earth Sciences 3715. BOFS Publication 207.

References

Agrawal, Y.C., I.N. McCave, and J.B. Riley, Laser diffraction size analysis, in *Principles, Methods and Application of Particle Size Analysis,* edited by J.P.M. Syvitski, pp.119-128, Cambridge University Press, New York, 1991.

Allen, J.R.L., A theoretical and experimental study of climbing-ripple cross-lamination, with a field application to the Uppsola esker, *Geogr. Ann., 53A*, 157-187, 1971.

Andrews, J.T., and K. Tedesco, Detrital carbonate-rich sediments, northwestern Labrador Sea: Implications for ice-sheet dynamics and iceberg rafting (Heinrich) events in the North Atlantic, *Geology, 20,* 1087-1090, 1992.

Balsam, W.L., and F.W. McCoy, Atlantic sediments: glacial/interglacial comparisons, *Paleoceanography, 2,* 531-542, 1987.

Bird, A.A., G.L. Weatherly, and M. Wimbush, A study of the bottom boundary layer over the eastward scarp of the Bermuda Rise, *J. Geophys, Res., 87,* 7941-7954, 1982.

Bond, G., H. Heinrich, S. Huon, W.S. Broecker, L. Labeyrie, J. Andrews, J. McManus, S. Clasen, K. Tedesco, R. Jantschink, C. Simet, and K. Mieczyslawa, Evidence for massive discharges of icebergs into the glacial northern Atlantic, *Nature, 360,* 245-249, 1992.

Boulton, G.S., Sedimentary and sea level changes during glacial cycles and their control on glacimarine facies architecture, in *Glacimarine Environments: Processes and Sediments,* edited by J.A. Dowdeswell and J.D. Scourse, *Geol. Soc. London Spec. Publ., 53,* 15-52, 1990.

Bowden, K.F., The dynamics of flow on a submarine ridge, *Tellus, 12,* 418-426, 1960.

Bridge, J.S., Hydraulic interpretation of grain-size distributions using a physical model for bedload transport, *J. Sediment. Petrol., 51,* 1109-1124, 1981.

Bulfinch, D.L., and M.T. Ledbetter, Deep western boundary undercurrent delineated by sediment texture at base of North American continental rise, *Geo. Mar. Lett., 3,* 31-36, 1984.

Coakley, J.P., and J.P.M. Syvitski, SediGraph techniques, in *Principles, Methods and Application of Particle Size Analysis*, edited by J.P.M. Syvitski, pp. 129-142,Cambridge University Press, New York, 1991.

Corliss, B.H., D.G. Martinson, and T. Keffer, Late Quaternary deep-ocean circulation, *Geol. Soc. Am. Bull., 97,* 1106-1121, 1986.

Dade, W.B., and A.R.M. Nowell, Moving muds in the marine environment, in *Coastal Sediments '91 Proceedings Specialty Conference*pp. 54-71, American Society of Civil Engineers, New York, 1991.

Dade, W.B., A.R.M. Nowell, and P.A. Jumars, Predicting erosion resistance of muds, *Mar. Geol., 105,* 285-297, 1992.

Dickson, R.R., Global summaries and intercomparisons: Flow statistics from long-term current meter moorings, in *Eddies in Marine Science,* edited by A.R. Robinson, pp. 278-353, Springer-Verlag, New York, 1983.

Dickson, R.R., and I.N. McCave, Nepheloid layers on the continental slope west of Porcupine Bank, *Deep Sea Res., 33,* 791-818, 1986.

Drake, D.E., and D.A. Cacchione, Field observations of bed shear stress and sediment resuspension on continental shelves, Alaska and California, *Cont. Shelf Res., 6,* 415-429, 1986.

Driscoll, M.L., B.E. Tucholke, and I.N. McCave, Seafloor zonation in sediment texture on the Nova Scotian Lower Continental Rise, *Mar. Geol., 66,* 25-41, 1985.

Eittreim, S., E.M. Thorndike, and L. Sullivan, Turbidity distribution in the Atlantic Ocean, *Deep Sea Res., 23,* 1115-1127, 1976.

Embley, R.W., and R.D. Jacobi, Distribution and morphology of large submarine slides and slumps on Atlantic continental margins, *Mar. Geotechnol., 2,* 205-228, 1977.

Ezer, T., and G.L. Weatherly, Small-scale spatial structure and long-term variability of near-bottom layers in the HEBBLE area, *Mar. Geol., 99,* 319-328, 1991.

Fillon, R.H., Northwest Labrador Sea stratigraphy, sand input and paleoceanography during the last 160,000 years, in *Quaternary Environments: the Eastern Canadian Arctic, Baffin Bay and West Greenland,* edited by J.T. Andrews, pp. 210-247, Allen and Unwin, Winchester, Mass., 1985.

Georgi, D.T., Circulation of bottom waters in the southwestern South Atlantic, *Deep-Sea Res., Part A 28,* 959-979, 1981.

Gross, T.F., and A.J. Williams, A deep-sea sediment transport storm, *Nature, 331,* 518-521, 1988.

Gross, T.F., and A.J. Williams, Characterization of deep-sea storms, *Mar. Geol., 99,* 281-301, 1991.

Haskell, B.J., and T.C. Johnson, Surface sediment response to deep water circulation on the Blake Outer Ridge, Western North Atlantic: palaeoceanographic implications, *Sediment. Geol., 82,* 133-144, 1993.

Haskell, B.J., T.C. Johnson, and W.J. Showers, Fluctuations in deep western North Atlantic circulation on the Blake Outer Ridge during the last deglaciation, *Paleoceanography, 6,* 21-31, 1991.

Hogg, N.G., R.S. Pickart, R.M. Hendry, and W.J. Smethie, The Northern Recirculation Gyre of the Gulf Stream, *Deep Sea Res., 33,* 1139-1165, 1986.

Holland, W.R., and P.B. Rhines, An example of eddy-induced ocean circulation, *J. Phys. Oceanogr., 10,* 1010-1031, 1980.

Hollister, C.D., and B.C. Heezen, Geologic effects of ocean bottom currents: Western North Atlantic, in *Studies in Physical Oceanography*, vol. 2, edited by A.L. Gordon, pp. 37-66, Gordon and Breach, New York, 1972.

Hollister, C.D. and I.N. McCave, Sedimentation under deep-sea storms, *Nature, 309,* 220-225, 1984.

Hunt, J.R., Particle aggregate breakup by fluid shear, in *Estuarine Cohesive Sediment Dynamics,* edited by A.J. Mehta, pp. 85-109, Springer-Verlag, New York, 1986.

James, A.E., and D.J.A. Williams, Flocculation and rheology of kaolinite/quartz suspensions, *Rheol. Acta, 21,* 176-183, 1982.

Johnson T.C., E.L. Lynch, W.J. Showers, and N.C. Palczuk, Pleistocene fluctuations in the western boundary undercurrent on the Blake Outer Ridge, *Paleoceanography, 3,* 191-207, 1988.

Jones, K.P.N. Studies of fine-grained, deep-sea sediments, Ph.D. thesis, 248 pp.,Univ. of Cambridge, Cambridge, Engl., 1988.

Jones, K.P.N., I.N. McCave, and P.D. Patel, A computer-interfaced SediGraph for modal size analysis of fine-grained sediment, *Sedimentology, 35,* 163-172, 1988.

Krone, R.B., Flume studies of the transport of sediment in estuarial shoaling processes, report, 110 pp., Hydraul. Eng. and Sanit. Eng. Res. Lab. Univ. of Calif., Berkeley, 1962.

Lampitt, R.S., Evidence for the seasonal deposition of detritus to the deep-sea floor and its subsequent resuspension, *Deep Sea Res., 32,* 885-897, 1985.

Ledbetter, M.T., Fluctuations of Antarctic Bottom Water in the Vema Channel during the last 160,000 years, *Mar. Geol., 33,* 71-89, 1979.

Ledbetter, M.T., A late Pleistocene time-series of bottom-current speed in the Vema Channel, *Palaeogeogr. Palaeoclimatol. Palaeoecol., 53,* 97-105, 1986.

Ledbetter, M.T., and W.L. Balsam, Paleoceanography of the Deep Western Boundary Undercurrent on the North American continental margin for the past 25,000 yr, *Geology, 13,* 181-184, 1985.

Ledbetter, M.T., and A. Klaus, Influence of bottom currents on sediment texture and sea-floor morphology in the Argentine Basin, in Geology and Geochemistry of Abyssal Plains, edited by P.P. Weaver and J. Thomson, *Geol. Soc. London Spec. Publ., 31,* 23-31, 1987.

Lonsdale, P., Sediment Drifts of the Northwest Atlantic and their relationship to the observed abyssal currents, *Bull. Inst. Geol. Bassin Aquitaine, 31,* 141-149, 1982.

Lonsdale, P., and B. Malfait, Abyssal dunes of foraminiferal sand on the Carnegie Ridge, *Geol. Soc. Am. Bull., 85,* 1697-1712, 1974.

Manighetti, B., and I.N. McCave, Late glacial and Holocene palaeocurrents around South Rockall Bank, northeastern Atlantic, *Paleoceanography,* this issue.

Mantz, P.A., Incipient transport of fine grains and flakes - An extended Shields diagram, *J. Hydraul. Div. Am. Soc. Civ. Eng., 103,* 601-615, 1977.

Mantz, P.A., Bedforms produced by fine, cohesionless, granular and flakey sediments under subcritical water flows, *Sedimentology, 25,* 83-103, 1978.

Massé, L., Sedimentation oceanique profonde au Quaternaire. Flux sedimentes et paleocirculations dans l'Atlantique sud-ouest: Bassin sud-Brezilien et prisme d'accretion sud-Barbade. Ph.D. thesis, 339 pp., Univ. Bordeaux I, France, 1993.

McCave, I.N., Erosion and deposition by currents on submarine slopes, *Bull. Inst. Geol. Bassin Aquitaine, 31,* 47-55, 1982.

McCave, I.N., Particulate size spectra, behaviour and origin of nepheloid layers over the Nova Scotian Continental Rise, *J. Geophys. Res., 88,* 7647-7666, 1983.

McCave, I.N., Erosion, transport and deposition of fine grained marine sediments, in Fine-Grained Sediments: Deep Sea Processes and Facies, edited by D.A.V. Stow and D.J.W. Piper, *Geol. Soc. London Spec. Publ., 15,* 35-69, 1984.

McCave, I.N., Sedimentology and stratigraphy of box cores from the HEBBLE site on the Nova Scotian Continental Rise, *Mar. Geol., 66,* 59-89, 1985.

McCave, I.N., Stirrings in the abyss, *Nature, 331,* 484, 1988.

McCave, I.N., and S.A. Swift, A physical model for the rate of deposition of fine-grained sediment in the deep sea, *Geol. Soc. Am. Bull., 87,* 541-546, 1976.

McCave, I.N., and J.P.M. Syvitski, Principles and methods of geological particle size analysis, in *Principles, Methods and Application of Particle Size Analysis,* edited by J.P.M. Syvitski, pp. 3-21, Cambridge University Press, New York, 1991.

McCave, I.N., P.F. Lonsdale, C.D. Hollister, and W.D. Gardner, Sediment transport over the Hatton and Gardar contourite drifts, *J. Sediment. Petrol., 50,* 1049-1062, 1980.

Middleton, G.V., Hydraulic interpretation of sand size distributions, *J. Geol., 84,* 405-426, 1976.

Migniot, C., Etude des propriétés physiques de différents sédiments trés fins et de leur comportement sous des actions hydrodynamiques, *Houille Blanche, 7,* 591-620, 1968.

Miller, M.C., and P.D. Komar, The development of sediment threshold curves for unusual environments (Mars) and for inadequately studied materials (foram sands), *Sedimentology, 24,* 709-721, 1977.

Miller M.C., I.N. McCave, and P.D. Komar, Threshold of sediment motion under unidirectional currents. *Sedimentology, 24,* 507-527, 1977.

Okada, H., and A. McIntyre, Modern coccolithophores of the Pacific and North Atlantic Oceans, *Micropalaeontology, 23,* 1-55, 1977.

Oser, R.K., Sedimentary components of northwest Pacific pelagic sediments, *J. Sediment. Petrol., 42,* 461-467, 1972.

Parkin, D.W., Trade-winds during the glacial cycles, *Proc. R. Soc. London Ser.A, 337,* 73-100, 1974.

Partheniades, E., Erosion and deposition of cohesive soils, *J. Hydraul. Div. Am. Soc. Civ. Eng., 91,* 105-139, 1965.

PeakFit, Peak Analysis Software, Jandel Scientific, Erkrath, Germany, 1990.

Pond, S., and G.L. Pickard, *Introductory Dynamical Oceanography,* 2nd ed., 329 pp., Pergamon, New York, 1983.

Rees, A.I., Some flume experiments with a fine silt, *Sedimentology, 6,* 209-240, 1968.

Richardson, M.J., M. Wimbush, and L.A. Mayer, Exceptionally strong near-bottom flows on the continental rise of Nova Scotia, *Science, 213,* 887-888, 1981.

Robinson, S.G., and I.N. McCave, Orbital forcing of bottom-current enhanced pelagic sedimentation on Feni Drift, NE Atlantic, during the mid-Pleistocene, *Paleoceanography, 9,* 943-972, 1994.

Russel, W.B., Review of the role of colloidal forces in the rheology of suspensions, *J. Rheol., 24,* 287-317, 1980.

Sandwell, D.T., and B. Zhang, Global mesoscale variability from the GEOSAT exact repeat mission: Correlation with ocean depth, *J. Geophys. Res., 94,* 17,971-17,984, 1989.

Schmitz, W.J., Abyssal eddy kinetic energy in the North Atlantic, *J. Mar. Res., 42,* 509-536, 1984a.

Schmitz, W.J., Abyssal eddy kinetic energy levels in the

western North Pacific, *J. Phys. Oceanogr., 14,* 198-201, 1984b.

Schmitz, W.J., Observations of the vertical structure of the eddy field in the Kuroshio Extension. *J. Geophys. Res., 89,* 6355-6364, 1984.

Schönfeld, J., and H.R. Kudrass, Hochfrequente Turbiditsedimentation in der Sulu-see (Phillipinen), *Z. Dtsch. Geol. Ges., 142,* 179-197, 1991.

Self, R.F.L., A.R.M. Nowell, and P.A. Jumars, Factors controlling critical shears for deposition and erosion of individual grains, *Mar. Geol., 86,* 181-199, 1989.

Shackleton, N.J., Oxygen isotopes, ice volume and sea level, *Quat. Sci. Rev., 6,* 183-190, 1987.

Shackleton, N.J., A. Berger, and W.R. Peltier, An alternative astronomical calibration of the lower Pleistocene timescale based on ODP Site 677, *Trans. R. Soc. Edinburgh Earth Sci., 81,* 251-261, 1990.

Sheridan, M.F., K.H. Wohletz, and J. Dehn, Discrimination of grain-size subpopulations in pyroclastic deposits, *Geology, 15,* 367-370, 1987.

Shum, C.K., R.A. Werner, D.T. Sandwell, B.H. Zhang, R.S. Nerem, and B.D. Tapley, Variations of global mesoscale eddy energy observed from GEOSAT, *J. Geophys. Res., 95,* 17,865-17,876, 1990.

Singer, J., J.B. Anderson, M.T. Ledbetter, K.P.N. Jones, I.N. McCave, and R. Wright, The assessment of analytical techniques for the analysis of fine-grained sediments, *J. Sediment. Petrol., 58,* 534-543, 1988.

Southard, J.B., and L.A. Boguchwal, Bed configurations in steady unidirectional water flows, 2, Synthesis of flume data, *J. Sediment. Petrol., 60,* 658-679, 1990.

Stein, R., Rapid grain-size analyses of clay and silt fraction by Sedigraph 5000D: Comparison with Coulter Counter and Atterberg methods, *J. Sediment. Petrol., 55,* 590-593, 1985.

Syvitski, J.P.M. (Ed.), *Principles, Methods and Application of Particle Size Analysis,* 368 pp., Cambridge University Press, New York, 1991.

Thorpe, S.A., Current and temperature variability on the continental slope, *Phil. Trans. R. Soc. London Ser.A, 323,* 471-517, 1987.

Thorpe, S.A., and M. White, A deep intermediate nepheloid layer, *Deep Sea Res., 35,* 1665-1671, 1988.

Unsold, G., Der Transportbeginn rolligen Sohlmaterials in gleichformigen turbulenten Stromungen: eine kritische Uberprufung der Shields-Funktion und ihre experimentelle Erweiterung auf feinstkörnige, nicht-bindige Sedimente, Doctoral dissertation, 145 pp, Univ. of Kiel, Kiel, Germany, 1982.

van Andel, T.H., Texture and dispersal of sediments in the Panama Basin, *J. Geol., 81,* 434-457, 1973.

Wang H., and I.N. McCave, Distinguishing climatic and current effects in mid-Pleistocene sediments of Hatton and Gardar Drifts, NE Atlantic, *J. Geol. Soc. London, 147,* 373-383, 1990.

Warren, B.A., Transpacific hydrographic sections at Lats. 43°S and 28°S: The SCORPIO Expedition, II, Deep Water, *Deep Sea Res., 20,* 9-38, 1973.

Warren, B.A., Deep circulation of the world ocean, in *Evolution of Physical* Oceanography, edited by B.A. Warren and C. Wunsch, pp. 6-41, MIT Press, Cambridge, Mass., 1981.

Weatherly, G.L., An estimate of bottom frictional dissipation by Gulf Stream fluctuations, *J. Mar. Res., 42,* 289-301, 1984.

Weatherly, G.L., and E.A. Kelley, 'Too cold' bottom layers at the base of the Scotian Rise, *J. Mar. Res., 40,* 985-1012, 1982.

Weatherly, G.L., and E.A. Kelley, Two views of the cold filament, *J. Phys. Oceanogr., 15,* 68-81, 1985.

Weatherly, G.L., and M. Wimbush, Near-bottom speed and temperature observations on the Blake-Bahama outer ride, *J. Geophys. Res., 85,* 3971-3981, 1980.

Weaver, C.E., *Clays, Muds and Shales,* 810 pp., Elsevier, New York, 1989.

Weaver, P.P.E., and J. Thomson, Calculating erosion by deep-sea turbidity currents during initiation and flow, *Nature, 364,* 136-138, 1993.

Weaver, P.P.E., R.G. Rothwell, J. Ebbing, D. Gunn, and P.M. Hunter, Correlation, frequency of emplacement and source directions of megaturbidites on the Madeira Abyssal Plain, *Mar. Geol., 109,* 1-20, 1992.

Weltje, G.J., and P.L. de Boer, Astronomically induced palaeoclimatic oscillations reflected in Pliocene turbidite deposits on Corfu (Greece): Implications for the interpretation of higher order cyclicity in ancient turbidite systems, *Geology, 21,* 307-310, 1993.

Welsh, E.B., N.G. Hogg, and R.M. Hendry, The relationship of low-frequency deep variability near the HEBBLE site to Gulf Stream fluctuations, *Mar. Geol., 99,* 303-317, 1991.

Zlotnicki, V., L-L. Fu, and W. Patzert, Seasonal variability in global sea level observed with GEOSAT altimetry, *J. Geophys. Res., 94,* 17,959-17,969, 1989.

I.N. McCave, and B. Manighetti, Department of Earth Sciences, University of Cambridge, Downing Street, Cambridge CB2 3EQ, England, U.K.(e-mail: mccave @esc.cam.ac.uk)

S.G. Robinson, Department of Environmental and Geophysical Sciences, Manchester Metropolitan University, John Dalton Building, Chester Street, Manchester, M1 5GD, England, U.K.

(Received November 23, 1993; revised May 4, 1994; accepted November 16, 1994.)